UNIVERSITY OF BIRMINGHAM
University of Birmingham Research at Birmingham

GIGA: a versatile genetic algorithm for free and supported clusters and nanoparticles in the presence of ligands

Jäger, Marc; Schäfer, Rolf; Johnston, Roy L

DOI:
10.1039/c9nr02031d

License:
None: All rights reserved

Document Version
Peer reviewed version

Citation for published version (Harvard):
Jäger, M, Schäfer, R & Johnston, RL 2019, 'GIGA: a versatile genetic algorithm for free and supported clusters and nanoparticles in the presence of ligands', *Nanoscale*, vol. 11, no. 18, pp. 9042-9052. https://doi.org/10.1039/c9nr02031d

Link to publication on Research at Birmingham portal

Publisher Rights Statement:
Checked for eligibility: 20/05/2019
10.1039/C9NR02031D

General rights
Unless a licence is specified above, all rights (including copyright and moral rights) in this document are retained by the authors and/or the copyright holders. The express permission of the copyright holder must be obtained for any use of this material other than for purposes permitted by law.

•Users may freely distribute the URL that is used to identify this publication.
•Users may download and/or print one copy of the publication from the University of Birmingham research portal for the purpose of private study or non-commercial research.
•User may use extracts from the document in line with the concept of 'fair dealing' under the Copyright, Designs and Patents Act 1988 (?)
•Users may not further distribute the material nor use it for the purposes of commercial gain.

Where a licence is displayed above, please note the terms and conditions of the licence govern your use of this document.

When citing, please reference the published version.

Take down policy
While the University of Birmingham exercises care and attention in making items available there are rare occasions when an item has been uploaded in error or has been deemed to be commercially or otherwise sensitive.

If you believe that this is the case for this document, please contact UBIRA@lists.bham.ac.uk providing details and we will remove access to the work immediately and investigate.

Download date: 25. Apr. 2024

Journal Name

ARTICLE TYPE

Cite this: DOI: 10.1039/xxxxxxxxxx

GIGA: A Versatile Genetic Algorithm for Free and Supported Clusters and Nanoparticles in the Presence of Ligands†

Marc Jäger,*[a] Rolf Schäfer,[a] and Roy L. Johnston*[b]

Received Date
Accepted Date

DOI: 10.1039/xxxxxxxxxx

www.rsc.org/journalname

We present a versatile parallelised genetic algorithm, which is able to perform global optimisation from first principles for pure and mixed free clusters in the gas phase, supported on surfaces or in the presence of one or several atomic or molecular species (ligands or adsorbates). The genetic algorithm is coupled to different quantum chemical software packages in order to permit a large variety of methods for the global optimisation. The genetic algorithm is also capable of optimising different electronic spin multiplicities explicitly, which allows global optimisation on several potential energy hyper-surfaces in parallel. We employ the genetic algorithm to study ligand-passivated clusters $[Cd_3Se_3(H_2S)_3]^+$ and to investigate adsorption of $[Pt_6(H_2O)_2]^+$ supported on graphene. The explicit consideration of the electronic spin multiplicity during global optimisation is investigated for nanoalloy clusters Pt_4V_2.

1 Introduction

In modern nanoscience, great efforts are being made to globally optimise nanosystems, such as clusters, to find the geometry with the overall lowest energy, the so-called global minimum (GM).[1–5] On the one hand, global optimisation (GO) of nanoparticles (NPs) plays an important role in rational materials design, in order to tailor material properties for future applications. On the other hand, the GM is, from a thermodynamic point of view, the most stable structure (at $T = 0$ K) and often the most likely candidate to be formed in an experiment.[5] Within the Born-Oppenheimer (BO) approximation, each local minimum on the potential energy surface represents a stable structural isomer. The number of minima rises exponentially with the number of atoms in the cluster and for multielemental NPs it is even more complicated due to inequivalent permutational isomers or so-called "homotops"[6]. Hence, sophisticated search methods are essential for the GO of nanosystems. Well established algorithms for the GO of clusters and NPs are: the genetic algorithm (GA), basin hopping (BH), particle swarm optimisation (PSO), artificial bee colony (ABC), simulated annealing, and the threshold algorithm. The reader is referred to the literature for more details on these global optimisation methods.[5,7–11]

Genetic algorithms have been successfully applied to the global optimisation of many clusters and NPs.[1,2,5,12] The origin of the GA presented here is the Birmingham Cluster Genetic Algorithm (BCGA), a Lamarckian-type GA developed for the GO of free pure and mixed clusters using plane-wave density functional theory (pw-DFT) or empirical potentials (EPs).[5,13] Subsequently, a surface mode (S-BCGA) was introduced.[14] The next step was the implementation of the pool concept, which enables massive parallelisation of the GA.[3,4] In the pool mode, many independent GA instances act on a global data base, the pool, which contains the current lowest energy cluster structures. This concept was first introduced into the original Fortran code (pool-BCGA)[4] and then rewritten in Python as the Birmingham Parallel Genetic Algorithm (BPGA)[3], which was coupled to the Vienna ab initio simulation package (VASP)[15–18]. The most recent descendant of the BCGA is the Mexican Enhanced Genetic Algorithm (MEGA),[19] which was redesigned to make the code more efficient and flexible and to provide a detailed history for later analysis. MEGA also uses structural distance criteria in order to maintain geometric diversity in the pool database.

Here an advanced version of MEGA is introduced, which is able to perform GO for clusters in the presence of one or several atomic or molecular species, which can be ligands or adsorbates (e.g. reactants and intermediates in catalytic reactions). This can be achieved for free or supported clusters. We have extended MEGA

[a] Technische Universität Darmstadt, Eduard-Zintl Institut für Anorganische und Physikalische Chemie, Alarich-Weiss-Straße 8, 64287 Darmstadt, Germany. E-mail: jaeger@cluster.pc.chemie.tu-darmstadt.de

[b] University of Birmingham, School of Chemistry, Edgbaston, Birmingham B15 2TT, United Kingdom. E-mail: r.l.johnston@bham.ac.uk

† Electronic Supplementary Information (ESI) available: [details of any supplementary information available should be included here]. See DOI: 10.1039/b000000x/

‡ Additional footnotes to the title and authors can be included *e.g.* 'Present address:' or 'These authors contributed equally to this work' as above using the symbols: ‡, §, and ¶. Please place the appropriate symbol next to the author's name and include a `\footnotetext` entry in the the correct place in the list.

to include the GO of clusters in the presence of ligands or adsorbates and have implemented additional optimisation modes. Some changes of the GO of bare clusters, such as the calculation of moment of inertia eigenvalues for structural comparison are also implemented. The code has been coupled to several quantum chemical software packages. Following the nomenclature of MEGA, the new GA has been named the German Improved Genetic Algorithm (GIGA). For a thorough analysis of the GIGA output, a post-GA analysis tool was developed, which is introduced in the Electronic Supplementary Information.

Section 2 describes the methodology, especially the implementation of ligand optimisation. In section 3 we report the application of GIGA to the GO of three distinct systems: $[Cd_3Se_3(H_2S)_3]^+$; $[Pt_6(H_2O)_2/\text{graphene}]^+$; and Pt_4V_2.

2 Methodology

The motivation for the design of GIGA is the development of a versatile GA which can perform the GO of free and supported clusters in the presence of ligands and adsorbates. This will help to support experimental studies, such as gas-phase pick-up experiments and cluster catalysis experiments, where clusters are deposited on a surface and then exposed to reactant molecules. GIGA is able to handle different ligand types simultaneously. As well as VASP, GIGA is coupled to Quantum Espresso (QE)[20] and NWChem,[21] in order to expand the range of quantum chemical methods for the local optimisations and to include open-source software packages. The coupling to NWChem enables the use of atom-centered wavefunction-based DFT or ab initio methods such as Configuration Interaciton (CI) or Coupled Cluster (CC) in the GO. It also allows the explicit consideration of the electronic spin multiplicity during the GO.

The innovations in GIGA are described in detail below.

2.1 Spin optimisation

In the current implementation, a list of possible electronic spin multiplicities (SM) and a frequency list, which contains the probabilities for the realisation of these spin multiplicities is passed to the GA. According to the predefined SM probabilities, the SM of each generated cluster is randomly chosen, so that during GO the overall GM, i.e the cluster structure and the corresponding SM, can be searched simultaneously. A spin seeding option has also been implemented. In this mode, all structures in the pool are copied and, for each possible SM, a local optimisation is performed for every cluster geometry in the pool. This spin seeding option can be applied to the GM search after every m generated structures (typically $m > 100$) to speed up the overall search and to avoid stagnation of the spin state.

2.2 Three-parent crossover

A new crossover option, the so-called three-parent crossover (3PC) is implemented, which also helps to increase the pool diversity in order to avoid stagnation. In the 3PC operation a similar scheme to the Deaven-Ho cut and splice operator[22] is applied, but three clusters from the pool database are selected according to their fitness. They are randomly rotated and each one is sliced by two cutting planes. To generate a single offspring, complementary sections are combined from the three parents. The probability of the occurrence of the 3PC operation can be individually adjusted for each GA instance working on the pool database.

2.3 Optimisation of cluster-bound ligands or adsorbates

To facilitate efficient GO of clusters in the presence of ligands or adsorbates, which are bound to the cluster, the atoms of the cluster and those of the ligands or adsorbates have to be treated separately. In the following, the term ligand represents any cluster-bound atoms and molecules as chemical ligands and adsorbates.

First, an initial structure for the cluster is generated as in the previous GA versions.[3,19] The origin of the cluster coordinate system is the center of mass (CoM) of the cluster. Initial ligand structures, stored in external geometry files, are read into the program. The atoms of each ligand are labelled by a unique ligand-identification-number (ligand-ID) to ensure, even in complex systems, that each atom is retained in the correct ligand entity. There are three different operations (Random 1, Random 2 and Random 3) for randomly placing the ligands around the cluster. There is also an option to bias the orientation of the ligand towards the cluster. For each atom in the ligand, a probability is defined for that atom being bound to the cluster. After placing the ligand (or adsorbate) on the cluster, a ligand atom is selected according to the probability list and then a biased rotation takes place. This rotates the ligand so that the selected atom has the smallest distance to the CoM of the cluster and thus forms a chemical bond to one or more cluster atoms. After the initial cluster structure and ligand positions and orientations have been generated, they are passed to the selected quantum chemical software package for local energy minimisation. This procedure is repeated until the pool is filled.

The evolutionary operators of crossover and mutation can be applied simultaneously to ligand atoms and cluster atoms, with the constraint that the chemical bonds within each ligand are retained. Therefore, a transformation of the ligand structure is applied in advance, whereby each ligand is reduced to its individual bonding atom (that is the ligand atom which is closest to the cluster), before applying any mutation or crossover operator. The initial atomic positions and other information such as ligand-IDs are stored in an internal data base. This substitution allows the ligands to be treated in the same way as cluster atoms, irrespective of their size. Subsequently, the evolutionary operators are applied to the cluster-ligand structure to produce a new cluster-ligand descendant (offspring or mutant). The database is updated with the new positions of the substituted ligand atoms and a re-substitution operation is applied to obtain all the final atomic position of each ligand in the descendant. For the crossover operations, the Deaven-Ho cut-and-splice operator[22] is employed and a relabelling method for the final ligand-IDs is applied. In Figure 1, the ligand substitution and re-substitution process is shown for the crossover operation.

We have also defined new mutation operations which leave the cluster structure unchanged but modify the ligand positions and orientations. These mutations take into account the num-

This journal is © The Royal Society of Chemistry [year]

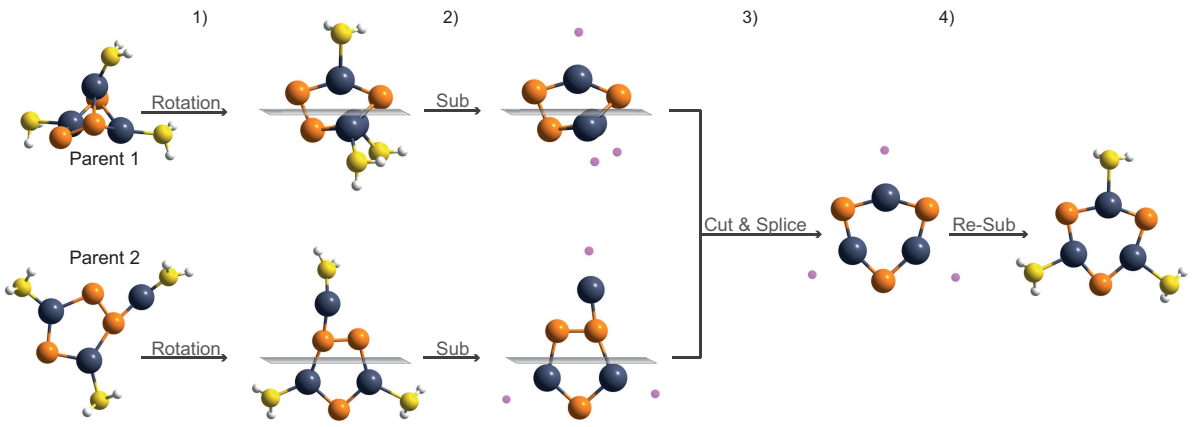

Fig. 1 The ligand substitution and re-substitution process as applied to the crossover operation. Two clusters are randomly selected: 1) a random rotation is executed; 2) each ligand is substituted by a single dummy atom at the position of its cluster binding atom; 3) the cut-and-splice- crossover operation is applied; 4) re-substitution of the ligand structures.

ber of atoms within each ligand and the number of different ligand species. In order to obtain a realistic initial bond length between the cluster and the ligands, the atomic radii r for all atoms are considered, as well as the overall ligand size. A good initial position is achieved if the distance d between the ligand bonding atom and the nearest cluster atom satisfies the condition: $0.9 \cdot (r_{\text{lig}} + r_{\text{clus}}) \leq d \leq 1.1 \cdot (r_{\text{lig}} + r_{\text{clus}})$. After each evolutionary operation, the whole cluster ligand structure is examined with respect to the atomic positions.

The new ligand mutations, which are shown in Fig. 2 and Fig 3, are:

- **Random 1**: One atom of the cluster is randomly selected and the ligand is randomly rotated and placed close to the chosen cluster atom, taking into account the ligand size and the atomic radius of the chosen cluster atom.
- **Random 2**: The ligand is randomly rotated and placed at the CoM of the cluster, then an arbitrary directional vector is calculated and the ligand is translated in this direction until there is no overlap between the cluster and ligand atoms.
- **Random 3**: A sphere is calculated, with its radius proportional to the cumulated radii of all cluster atoms and the sizes of the ligands. An arbitrary point p within the sphere is selected and the ligand is randomly rotated and placed so that its centroid corresponds to p. Subsequently, the previously described distance check is applied.
- **Full rotation**: All ligands are rotated around the cluster core by the same arbitrary angles maintaining the same distance of each individual ligand to the CoM of the cluster.
- **Partial rotation**: Only 30% of all ligands are rotated around the cluster.
- **Bond rotation**: One ligand is rotated through an arbitrary angle around the cluster-ligand bond (only for non-linear molecules)
- **Full new orientation**: All ligands are randomly reoriented (randomly rotated) so that their centroid is preserved (only for molecules). In the final orientation the ligand-cluster bonding may be changed.
- **Partial new orientation**: Only 30% of the ligands (only for molecules) are selected and randomly reoriented.
- **Full biased orientation**: All ligands are reoriented (rotated) relative to the cluster such that another ligand atom is bound to the cluster. This ligand atom is chosen beforehand according to a predefined probability list (only for molecules and only if the biased mode is enabled).
- **Partial biased orientation**: As above, but with reorientation of only 30% of the ligands.
- **Inversion**: The positions of 30% of all ligands are inverted (i.e. the atomic coordinates of the chosen ligands are changed from (x,y,z) to (-x,-y,-z); only for non-chiral ligands).
- **Swap**: Two ligands are randomly selected and their positions are switched so that the centroid of one ligand corresponds to the centroid of the other, and vice versa. For molecules in the way, that the absolute orientation of the ligand atoms in the coordinate space remains the same (only for different ligand species)
- **Move**: 30% of all ligands are moved in an arbitrary direction and distance.
- **Rattle**: 70% of all ligands are shifted in an arbitrary direction, but the distance is in the order of their ligand size. Therefore, the magnitude of the shifting vector is in the range of zero and the distance between the most distant atoms in the ligand.

To investigate the lowest energy cluster-ligand structures, it must be ensured that each generated geometry exhibits intact lig-

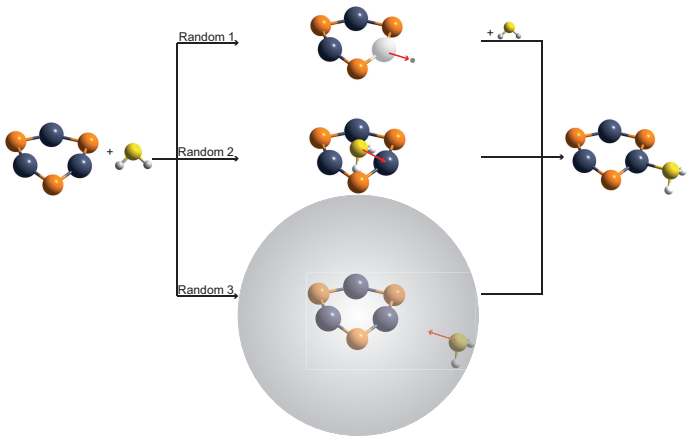

Fig. 2 Random placement ligand mutation operations. All three operations can randomly generate the same structure. Structures which show the ligand bridging to two nearby cluster atoms are more likely generated with Random 2 and Random 3, since no specific cluster atom is picked for the placing operation.

ands. Thus, it has to be noted that although each cluster geometry generated by the GA (before passing it to the QC software package) has only intact ligands, these chemical species could react with the cluster during local energy minimisation and the resulting structure has dissociated ligands, or the resulting energy minimised structure could also exhibit free ligands (ligands, which do not bind to the cluster core). Several different structural motifs obtained for the GO of $[Cd_3Se_3(H_2S)_3]^+$ are shown in the Supporting Information (cf. Fig. 2 and Fig. 3). Since only energy-minimised output structures are present in the pool database, which means that ligands could be dissociated, it must be guaranteed that GIGA always generates structures with intact ligands. Therefore a **ligand structure repair function** is implemented, which compares all bond length within each ligand of the selected ligand cluster geometry from the pool data base with the distances of its corresponding ligand template structure. If at least one intra-ligand distance differs by more than 20%, the ligand is replaced by the ligand template structure, such that its centroid and orientation are unchanged. In the NWChem software package, there is also the option to fix internal degrees of freedom of the ligands, such as bond lengths and bond angles in order to prevent overall reactions (ligand dissociation) during the local minimisation steps.

2.4 Free clusters

For the study of ligated clusters in the gas phase, two different generation modes (G-mode 1 and G-mode 2) are implemented. **G-mode 1**: The cluster is generated from scratch and the evolutionary operators are applied to both the ligand and cluster atoms. **G-mode 2 (pick-up mode)**: A template cluster structure (for example the GM of the bare cluster) is used as the starting point for every cluster-ligand complex and the ligands are attached and oriented on the cluster core in different ways. Hence, the evolutionary operations of mutation and crossover are only applied to the orientations and positions of the ligands. This mode is implemented to mimic pick-up experiments, in which the cluster is generated and then passed through a cell, in which it picks up the ligand molecules or atoms.[23] The pick-up mode may also help to reduce the computational time, since there are fewer possible structural alternatives.

With both modes it is possible to find bound ligand-cluster structures with intact ligands, reaction products with dissociated ligands, unbound ligands or unbound reaction products (cf. ESI Fig. 2 and Fig. 3). As already mentioned, dissociated and unbound ligands are possible during the local energy minimisation, however each new generated structure always starts with intact ligands.

2.5 Surface-supported clusters

By analogy to the ligand pick-up mode, a **soft-landing mode** for the GO of clusters on a surface slab is implemented to mimic low energy cluster deposition experiments. In this mode a template free cluster structure (for example the gas phase GM) is placed, with different randomly generated orientations close to the surface and is then locally relaxed at the chosen level of theory.

Adsorbate implementations on deposited cluster structures can be performed in two ways (S-mode 1 and S-mode 2). **S-mode 1**: The cluster structure is generated from scratch (near the surface, using the same distance criteria regarding the smallest distance of the surface bonding atom and the nearest cluster atom as for the cluster core and ligands) and the evolutionary operators are applied to both the adsorbate and cluster atoms. **S-mode 2**: A template for the deposited cluster (for example the GM for the supported bare cluster) is used as the starting structure and the adsorbates are placed and oriented in different ways around the cluster (as in the pick-up mode for free clusters). The evolutionary operations of mutation and crossover are only applied to the orientations and positions of the adsorbates. This mode is implemented to mimic heterogeneous cluster catalysis experiments, in which first clusters are deposited on a surface and then this system is exposed to reactant molecules.

In both modes, it can be chosen either to relax the surface atoms during the local minimisation or to freeze them. As in the case of free clusters, in the course of local energy minimisation it is possible to find bound adsorbate-cluster structures with intact adsorbates, reaction products with dissociated adsorbates, unbound adsorbates or unbound reaction products.

3 Results and discussion

3.1 Ligated free clusters

Quantum dots (QDs) of II-VI semiconductor clusters, such as CdSe are extensively studied systems due to their intriguing optoelectronic properties, which can be tuned by varying the particle size.[24–27] CdSe species are used in technical applications such as biomedical imaging, solar cells, lasers, light emitting diodes and displays.[28–32] Most synthesised CdSe QDs are colloidal, where ligands are attached to the CdSe core. It is well known that ligands can strongly affect the optoelectronic properties of a CdSe nanosystem.[33–38] To predict how optical properties are influenced by the attachment of the ligands, the system of interest must be modelled and compared to the bare cluster. Hence, it

This journal is © The Royal Society of Chemistry [year]

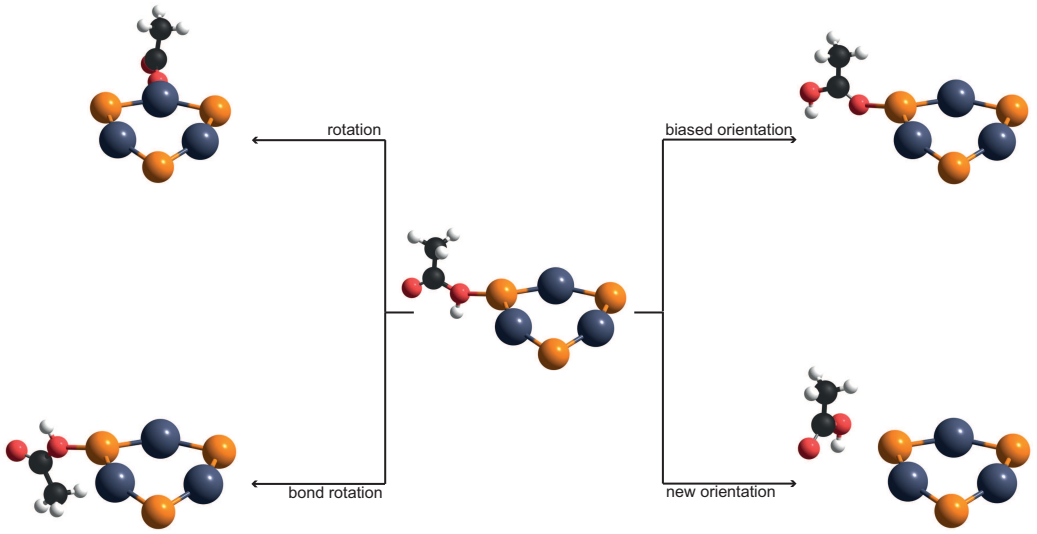

Fig. 3 Rotation and reorientation ligand mutation operations.

is essential to find the exact structures of the cluster-ligand complexes. Following this approach, the first step is the GO of the bare and ligated clusters of interest. Here we study $[Cd_3Se_3(H_2S)_3]^+$ as a test-system to probe the passivation effect of the simplest thiol-like ligand H_2S on the $Cd_3Se_3^+$ cluster. Our purpose is to investigate the lowest lying energy structures using the different modes of GIGA and to study the ligand influence on the geometrical and optical properties. To probe several options of GIGA, the GO of $[Cd_3Se_3(H_2S)_3]^+$ is performed in four different ways.

- **a**: G-Mode 1, cluster and ligands are both optimised from scratch using the software package QE for local minimisations with the PBE[39] xc functional and ultrasoft RRKJ-type[40] pseudopotentials. The plane-wave basis is truncated with a cut-off energy at 40 Ry and an electronic convergence criterion of 10^{-6} Ry.

- **b**: G-Mode 2 (pick-up mode), with the GM of bare $Cd_3Se_3^+$ as the cluster core structure using the software package QE with the same settings as in **a**.

- **c**: G-Mode 2 (pick-up mode), as for **b**, but using the software package NWChem with the PBE0[41] xc functional and employing the small atom-centered SBKJC-VDZ[42] basis functions with moderate convergence criteria (*medium grid*) and applying constraints on the ligand geometries: all angles and bond lengths of the ligands are kept constant during the local energy minimisations.

- **d**: G-Mode 2 (pick-up mode), as for **c**, but with no constraints on the ligand structures during the local minimisations.

First of all a GO of bare $Cd_3Se_3^+$ was performed in order to obtain the initial cluster structure for the pick-up modes (**b**, **c** and **d**). The 3PC implementation was also tested for $Cd_3Se_3^+$. Therefore, three GOs of bare $Cd_3Se_3^+$ are performed with different restrictions on the evolutionary operators: i) with both crossover types, ii) only with the "normal" crossover (with two parents) and iii) only with the 3PC. For all calculations, the software package VASP was employed for local geometry optimisations, applying the PBE xc functional and projected augmented wave (PAW)[43] pseudopotentials. The plane-wave basis set was truncated with a cut-off energy of 400 eV. The same lowest energy structure (D_{3h} symmetry) with alternating Cd and Se atoms was obtained for all three cases, which is in agreement with the previously proposed structure of $Cd_3Se_3^+$.[44] The GM is depicted in Figure 4.

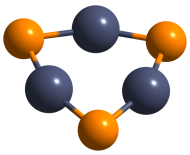

Fig. 4 GM structure of $Cd_3Se_3^+$ (D_{3h}) refined at the PBE0/cc-pVTZ-PP level of theory (Cd: dark blue atoms, Se: orange atoms).

For all options **a** - **d**, similar structures were found as the lowest lying energy candidates. These geometries only differ slightly due to the moderate convergence criteria during the GO, but all the lowest energy structures with intact ligands have the same cluster core as the $Cd_3Se_3^+$ GM, irrespective of the chosen optimisation option. In a further step, all lowest energy structures were relaxed at the higher PBE0/cc-pVTZ-PP[41,45,46] level of theory, using a high density grid and tight convergence criteria with the NWChem software package. This functional and basis set choice has previously been found to give a good description of CdSe clusters.[47] The resulting structures are shown in Figure 5. Three $[Cd_3Se_3(H_2S)_3]^+$ structures (Iso-I - Iso-III) were found which lie within an energy range of $\Delta E \leq 0.10$ eV. Iso-I and Iso-II have a single H_2S molecule bound to each Cd atom, while Iso-II has two H_2S molecules on one of the Cd atoms. Iso-IV shows ligand dissociation (chemical reaction took place during the local energy minimisation, resulting in a HS fragment bridging two Cd atoms and a H atom bound to one of the Se atoms) and exhibits the lowest energy. The isomers with intact H_2S ligands (Iso-I, Iso-II and Iso-

III) were obtained with all approaches, but the reaction product Iso-IV was found only with options **a** and **d**. The energetic ordering, and therefore, the GM, are dependent on the chosen level of theory. After refinement, two nearly degenerate geometries (Iso-I and Iso-II), which differ by less than 10^{-5} eV are obtained. They have the same structure, only differing in one Cd-S bond rotation. The energy-barrier to rotation is higher than 0.15 eV. The raw GA output analysis predicted Iso-III to be the GM for **a**, **b** and **c** and Iso-IV as the lowest energy structure for approach **d**. A more thorough analysis of all GA output data reveals that only Cd-S bonds (and no Se-S bonds) were found in case of geometries with intact ligand structures and many structural isomers, which only differ in rotations around the Cd-S bonds (as in Iso-I and Iso-II), were generated. An overview of the generated geometries during the GO of $[Cd_3Se_3(H_2S)_3]^+$ is shown in the ESI (Fig. 2 and Fig. 3). The fact that Se atoms do not bind to any intact ligand has also been found for several different ligands bound to very small CdSe clusters.[48] In all options, apart from **c**, some ligand dissociation reactions were observed, but at the plane-wave DFT method, they have much higher energies $\Delta E \geq 0.42$ eV with respect to the GM. Interestingly, the same lowest lying isomers of $[Cd_3Se_3(H_2S)_3]^+$ are obtained whether optimising the cluster-ligand complex from scratch or using the pick-up mode. These structures exhibit the same cluster core geometry as the GM of bare $Cd_3Se_3^+$. These results justify the use of the pick-up mode. Hence, GIGA can be used to find the best ligand passivated cluster structure.

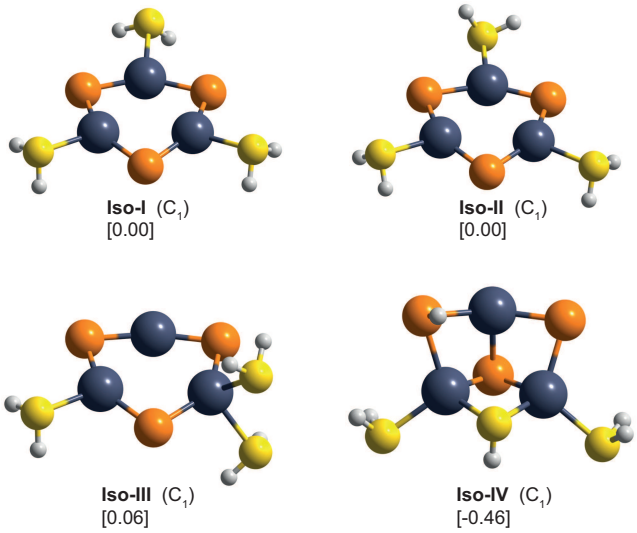

Fig. 5 Lowest lying $[Cd_3Se_3(H_2S)_3]^+$ isomers Iso-I - Iso-III (Cd: dark blue atoms, Se: orange atoms, H: white atoms, S: yellow atoms), which show the structural motif of the GM of $Cd_3Se_3^+$, and a reaction product (Iso-IV), the relative energies (in eV) are calculated at the PBE0/cc-pVTZ-PP level of theory and the point group symmetries are shown in parentheses.

To investigate the influence of ligands on the optoelectronic properties of the cluster, the optical absorption spectra were calculated using time dependent density functional theory (TDDFT) at the PBE0/cc-pVTZ-PP level of theory. The results are shown in Figure 6. In general, H_2S ligands cause a blue-shift of the absorption spectra and a significantly increased oscillator strength. A natural bond analysis (NBA) reveals (electron) charge transfer from the ligands to the cluster. In Iso-I, for example, 64.3% of the positive charge lies on the three H_2S ligands. This electron donating effect of the ligands has been also observed for neutral ligand passivated CdSe clusters.[33,36,49] It is impossible to distinguish between Iso-I and Iso-II using optical absorption data alone, due to the strong similarities in the optical absorption peaks. However, the absorption spectrum of Iso-III and (even more) the spectrum of Iso-IV strongly differ from the others and could be confirmed or excluded by a joint theoretical and experimental study.

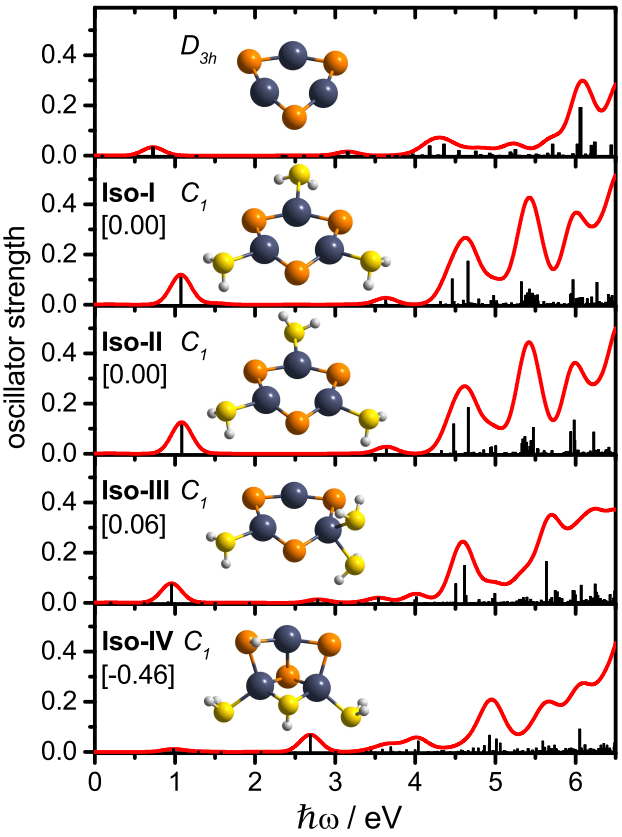

Fig. 6 Optical absorption spectra of bare $Cd_3Se_3^+$ and the lowest energy $[Cd_3Se_3(H_2S)_3]^+$ isomers after geometry refinement (Cd: dark blue atoms, Se: orange atoms, H: white atoms, S: yellow atoms), at the PBE0/cc-pVTZ-PP level of theory. The point group is specified in italic font and the relative energies in (eV) are given in square brackets. The calculated TDDFT line spectra (vertical black lines) are convoluted with Gaussian functions with a full width at half maximum of 0.3 eV (red lines).

3.2 Supported clusters with adsorbates

The investigation of supported platinum clusters and NPs is a very promising research field, due to their promising catalytic properties, which are caused by their high surface area and their remarkable high surface reactivity. Platinum NPs are used as catalysts in hydrogen and methanol fuel cells.[50,51] Pt clusters have also been studied because of their catalytic activity for water splitting,[52–54] the water gas shift reaction,[55] dehydrogenation[56] and many other chemical reactions[57–59]. It is desirable to investigate increasingly smaller NPs: 1) to use less of the expensive catalytically active material due to a higher overall surface area; 2) for ultrasmall (sub-nanometer) clusters quantum effects may signifi-

This journal is © The Royal Society of Chemistry [year]

cantly influence the catalytic activity. Another factor which may strongly affect the catalytic properties of the Pt NPs originates from the supporting substrate, since it can modify the electronic structure of the clusters. For Pt there have been several experimental and theoretical studies of the structures and properties of Pt clusters supported on graphene.[53,54,60–62] In order to gain a fundamental understanding of their catalytic properties knowledge of the exact structures of the supported NPs and the geometries of the adsorbates is of tremendous importance. For very small clusters, quantum effects must be adequately addressed by first principles electronic structure methods. In the following, a GO of the test system $[Pt_6/graphene]^+$ is performed in the presence of two water molecules and the lowest energy structures are identified using two different approaches. The graphene substrate consists of two layers with a total number of 224 atoms, which are kept fixed during all of the following simulations, in order to speed up the calculations. For all computations, the software package QE was employed, using the PBE[39] xc functional and ultrasoft RRKJ-type[40] pseudopotential for all species, since PBE has been proven to be a good choice for the description of Pt and graphene.[53,55,63–65] For all calculations, the plane-wave basis was truncated with a cut-off energy at 30 Ry and an electronic convergence criterion of 10^{-5} Ry was applied.

- **a**: S-Mode 1 Optimise $[Pt_6(H_2O)_2/graphene]^+$ from scratch, only the initial surface slab (graphene bilayer) and the initial H_2O ligand structures are pre-defined.

- **b**: Three step approach. Step 1: GO of free bare Pt_6^+. Step 2: GO of the Pt_6^+ GM structure on the surface slab (soft-landing mode). Step 3: (S-Mode 2) GO of $[Pt_6^+(H_2O)_2/graphene]^+$ using the GM of step 2 as the initial supported cluster structure.

For both approaches, the lowest energy structures were extracted with our GA-analysis tool and further refined using a higher kinetic energy cut-off (50 Ry) and a tighter electronic convergence criterion of 10^{-7} Ry.

Approach **a** can be compared with the growth of a Pt_6^+ cluster on a graphene surface in the presence of two water molecules. Here the water molecules interact with a probably metastable cluster structure and therefore can strongly influence the resulting geometry.

The best structures found using approach **a** are depicted in Figure 7. The predicted GM (Iso-I) shows water dissociation and both oxygens are bound on the same side of the Pt_6^+ cluster, which allows them to be further stabilised by forming a HOH–OH hydrogen bond. The dissociated H atom resides on a remote Pt atom. The Pt_6 structure exhibits four Pt vertex atoms, which are all accessible from three perpendicular directions, with a final vertex atom binding to the graphene surface, bridging a C-C bond. Iso-II is the lowest energy structure with two intact H_2O molecules. Only one H_2O is attached to a vertex atom of Pt_6 and the other (non-Pt-bound) H_2O species is stabilised by acting as a hydrogen bond acceptor to the bound water. Two Pt atoms of the cluster are bound to the surface, one coordinated to a single C atom and the other bridging a C-C bond.

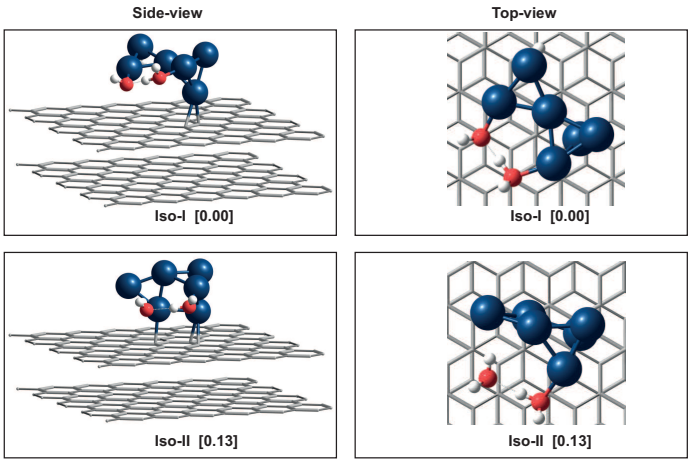

Fig. 7 Approach **a**: The lowest energy structure (Iso-I) of $[Pt_6(H_2O)_2/graphene]^+$ (Pt: blue atoms, O: red atoms, H: white atoms, surface: grey) and the lowest energy structure (Iso-II) with intact water molecules obtained with approach i) after refinement. All energies in brackets are given in eV relative to Iso-I

The lowest energy structures from procedure **b** are shown in Figure 8. This approach can be compared with soft-landed cluster deposition experiments and subsequent catalytic investigation of the supported cluster system.

The GM (structure A) for bare Pt_6^+ is a planar double square structure with D_{2h} symmetry, as has previously been predicted for neutral Pt_6.[66]. The next lowest lying structure is an octahedron (O_h symmetry), lying 0.30 eV higher than the GM. In step 2, the Pt_6^+ GM was used as the initial geometry employing the soft-landing mode of GIGA. The supported Pt_6^+ GM (structure B) shows the same cluster geometry as the GM of the isolated species (structure A). The planar double square geometry of Pt_6^+ is aligned perpendicular to the graphene surface with three Pt-C bonds singly bonded to the surface. The same structure was also found by performing an unbiased GO of Pt_6^+ on the graphene surface. Structure B is the initial structure for step 3, hence, the pick-up mode (S-Mode 2) was used to find the best overall structure of $[Pt_6(H_2O)_2/graphene]^+$. The lowest energy structure (Iso-III) shows ligand dissociation. The structure is a distorted version of structure B, with only one Pt atom attached to the surface, bridging a C-C bond. The undissociated H_2O molecule and the OH fragment are bound to two neighbouring Pt atoms and are stabilised by a HOH–OH hydrogen bond. Iso-IV is the lowest energy structure, with two intact H_2O adsorbates. The two Pt atoms at the interface are each connected to graphene by bridging C-C bonds. The water adsorbates are bound to opposite ends of the central Pt_2 unit. Iso-V is the lowest energy structure and has both intact water molecules and the identical Pt_6^+ structure as B. In this isomer, the oxygens of both ligands are bound to Pt vertex atoms, which are furthest apart.

Comparison of approaches **a** and **b** shows that lower energy-lying isomers were found using approach **a**, because no restrictions were imposed and the GA could explore the whole parameter space. For approach **b**, Iso-I and Iso-II could not be found due to restrictions on the cluster structure. In general, the best

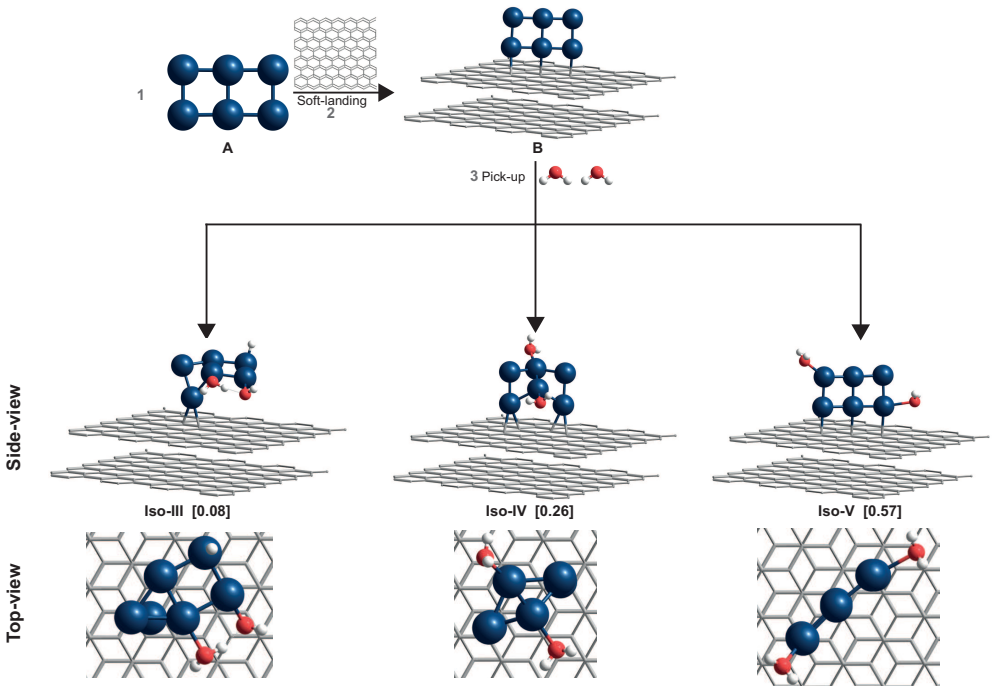

Fig. 8 Approach **b** (Pt: blue atoms, O: red atoms, H: white atoms, surface: grey): 1 The free Pt_6^+ GM structure (A); 2 the soft-landing GM of Pt_6^+ on graphene (structure B); 3 pick-up of 2 water molecules: the lowest energy structure (Iso-III), the lowest energy structure with intact water molecules (Iso-IV); and the best structure with geometry of structure B and intact water molecules (Iso-V) after refinement. All energies in brackets are given in eV relative to Iso-I.

solution may not be found by biasing global optimisation, but if it does, it can help to speed up the search process by reducing the parameter space. However, the lowest energy structures from approaches **a** and **b** (Iso-I and Iso-III) have some features in common: i) they exhibit water dissociation; ii) the adsorbed OH and H_2O species both form Pt-O bonds and are stabilised via a HOH–OH hydrogen bond; iii) the cluster is only bound to the surface by a single Pt atom, which bridges a C-C bond. Despite the similarities, it must be emphasised that different lowest energy structures were found for the two approaches **a** and **b**. Based on these observation, from a thermodynamic point of view, graphene supported Pt_6^+ clusters are highly reactive towards water dissociation and should be further investigated both experimentally and using more sophisticated quantum chemical methods. Furthermore, the supported cluster geometry is strongly influenced by the adsorbates, which has also been reported for other small Pt clusters based on theoretical and experimental investigations.[67,68] In order to be able to compare experiment and theory, the exact experimental conditions such as the overall experimental time scale and the temperature of the substrate are of enormous importance.

3.3 Explicit consideration of electronic spin

In this study, different spin multiplicities are explicitly included during the GO. This means that the GO has to take into account several electronic configurations, which leads to the search for the GM on several BO potential hypersurfaces. The test system is Pt_4V_2, to enable comparison with to study of Jennings and Johnston[69] on V-doped Pt clusters optimised directly at the DFT level, with subsequent geometry refinement at the PBE/def2-tzvp[39,70] level of theory for several spin multiplicities. In contrast to the previous study, which employed plane wave DFT during th GO, here atom-centered wave function based DFT is employed, using NWChem with the PBE0 xc functional and the small basis set SBKJC-vdz with medium grid. During the GO, the spin multiplicities (SM = 1, 3, 5, 7, 9) are taken into account explicitly. The lowest lying energy isomers have been refined at the PBE0/def2-tzvp[41,70] and the PBE/def2-tzvp levels of theory. The GM and spin multiplicities for these two xc functionals are shown in Figure 9. Compared to the previous study[69], no new low-lying isomers were found. However, depending on the xc functional the energy order changes dramatically, as well as the GM structure and favored spin multiplicity. In particular, the PBE0 functional, which contains 25 % exact Hartree-Fock exchange, favors the structure (Iso-I) with the higher SM (9). In order to make precise statements about the true GM, comparison with experimental data is necessary. However, to the best of our knowledge, to date there have been no experimental studies on Pt_4V_2.

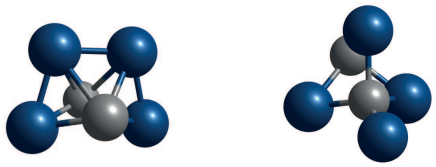

	Iso-I SM = 9	**Iso-II** SM = 3
ΔE(PBE0)/eV	0.00	0.97
ΔE(PBE)/eV	1.43	0.00

Fig. 9 Lowest energy isomers found for Pt_4V_2 (Pt: blue atoms, V: grey atoms) with spin multiplicities (SM) and relative energies at the PBE0/def2-tzvp and PBE/def2-tzvp levels of theory.

This journal is © The Royal Society of Chemistry [year]

4 Conclusions

We have demonstrated the capabilities of our versatile pool-based GA implementation GIGA. The new code extends the scope of GO to passivated NPs or the adsorption of chemical species on free and supported clusters. Different modes have been implemented, with the aim of better mimicking experimental approaches. The multifunctionality of GIGA has been presented, and its applicability to diverse systems has been highlighted. In this work, the GA was applied to three different test systems and several modes of the GA (for instance the pick-up mode) were tested. The first studied system was $Cd_3Se_3^+$ passivated with three H_2S ligands. All GA modes resulted in the same lowest energy isomers. Chemical reactions, such as ligand dissociation may also occur during the local minimisation step if there are no constraints imposed on the ligand intramolecular bond lengths. The overall GM shows D_{3h}-symmetry of the core cluster structure and each H_2S ligand is S-bound to a single Cd atom. The ligand influence on the optical absorption spectrum was also studied by means of TDDFT calculations. The presence of ligands results in a blue shift in the absorption spectrum and increased optical transition intensities, due to ligand to cluster charge transfer.

The GA was next tested for the adsorption of water on graphene supported Pt_6^+ clusters. Here, two different approaches were compared: **a**) GO of the whole system from scratch; and **b**) GO of free Pt_6^+, followed by GO of Pt_6^+ on the surface (using the soft landing mode) and finally the resulting GM was used in the pick-up mode for adsorbing the water molecules. In both cases, the lowest energy structures undergo water dissociation, though, different lowest energy structures are obtained for the two approaches. Lower lying energy structures were found with the direct GO from scratch since there are no restrictions on the parameter space. However, the results of both approaches must be compared with future experiments in order to make an accurate statement of which approach is more appropriate. Furthermore, in an experiment with a conducting substrate, Pt_6^+ is likely to become neutral (and could have another geometry), and therefore in general one should study both the cationic and neutral systems. Both systems can be analysed from scratch and with the soft-landing and pick-up mode, however in terms of neutral species for the soft-landing mode there are two alternatives: i) starting with the neutral free cluster or ii) using the charged free cluster with subsequent relaxation of the neutral system.

In the final example, the cluster's electronic spin was explicitly considered during the GO of Pt_4V_2. We found the same lowest energy isomers as proposed by Jennings and Johnston.[69] However, using the hybrid xc functional PBE0 with exact HF exchange, instead of PBE, the GM geometry and, hence, the preferred spin multiplicity changes significantly.

We have shown that GIGA can be applied to free pure and mixed clusters, passivated clusters, supported clusters and supported cluster with adsorbates. The GA is in principle also applicable to different optimisation problems such as protein ligand docking or solvated ions (using the pick-up mode). To make the GA more efficient, depending on the nanosystem to be studied, new system- or case-specific evolutionary operators (especially mutation operators) should be implemented and the ability to handle larger more flexible ligands. Regarding the quantum chemical local relaxation method, the relaxation of the surface slab should be allowed to obtain more precise results; the efficient treatment of hydrogen bonding including dispersion corrections should be employed or more sophisticated ab initio electronic structure methods should be used. Besides, the incorporation of empirical potentials should also be considered, in order to perform GO of larger passivated NPs. The efficiency of the GA could be significantly improved by combining it with sophisticated machine learning methods such as neural networks. In summary the GA presented here is a first step to an all-around optimisation tool for many different chemical systems and should help to better explain experimental results and to predict novel nanostructures for catalytic, optical or magnetic applications.

Conflicts of interest

There are no conflicts to declare.

Acknowledgements

We thank Jorge A. Vargas (UNAM, Mexico) for sharing the MEGA code. We acknowledge financial support from the Deutsche Forschungsgemeinschaft (grant SCHA 885/15-1) and COST action MP0903 (NANOALLOYS). MJ acknowledges a scholarship of the Merck'sche Gesellschaft für Kunst und Wissenschaft. The calculations were performed on the following HPC facilities: The University of Birmingham BlueBEAR facility and Thomas, the UK National Tier 2 High Performance Computing Hub in Materials and Molecular Modelling, which is partially funded by EPSRC (EP/P020194), via our membership of the UK's HEC Materials Chemistry Consortium funded by EPSRC (EP/L000202).

Notes and references

1 M. Jäger, R. Schäfer and R. L. Johnston, *Adv. Phys. X*, 2018, **3**, S100009.
2 S. Heiles and R. L. Johnston, *Int. J. Quantum Chem.*, 2013, **113**, 2091–2109.
3 J. B. Davis, A. Shayeghi, S. L. Horswell and R. L. Johnston, *Nanoscale*, 2015, **7**, 14032–14038.
4 A. Shayeghi, D. Götz, J. B. A. Davis, R. Schäfer and R. L. Johnston, *Phys. Chem. Chem. Phys.*, 2015, **17**, 2104–2112.
5 R. L. Johnston, *Dalt. Trans.*, 2003, 4193.
6 R. Ferrando, J. Jellinek and R. L. Johnston, *Chem. Rev.*, 2008, **108**, 845–910.
7 D. J. Wales and J. P. K. Doye, *J. Phys. Chem. A*, 1997, **101**, 5111–5116.
8 J. Lv, Y. Wang, L. Zhu and Y. Ma, *J. Chem. Phys.*, 2012, **137**, 084104.
9 J. Zhang and M. Dolg, *Phys. Chem. Chem. Phys.*, 2015, **17**, 24173–24181.
10 D. Hohl, R. O. Jones, R. Car and M. Parrinello, *J. Chem. Phys.*, 1988, **89**, 6823–6835.
11 S. Neelamraju, C. Oligschleger and J. C. Schön, *J. Chem. Phys.*, 2017, **147**, 152713.

12 C. J. Heard and R. L. Johnston, *Clust. Struct. Bond. React.*, Springer, Berlin, 2016, pp. 1–32.
13 S. Heiles, A. J. Logsdail, R. Schäfer and R. L. Johnston, *Nanoscale*, 2012, **4**, 1109.
14 C. J. Heard, S. Heiles, S. Vajda and R. L. Johnston, *Nanoscale*, 2014, **6**, 11777–11788.
15 G. Kresse and J. Furthmüller, *Phys. Rev. B*, 1996, **54**, 11169–11186.
16 G. Kresse and J. Hafner, *Phys. Rev. B*, 1994, **49**, 14251–14269.
17 G. Kresse and J. Hafner, *Phys. Rev. B*, 1993, **47**, 558–561.
18 G. Kresse and J. Furthmüller, *Comput. Mater. Sci.*, 1996, **6**, 15–50.
19 J. A. Vargas, F. Buendía and M. R. Beltrán, *J. Phys. Chem. C*, 2017, **121**, 10982.
20 P. Giannozzi, S. Baroni, N. Bonini, M. Calandra, R. Car, C. Cavazzoni, D. Ceresoli, G. L. Chiarotti, M. Cococcioni, I. Dabo, A. Dal Corso, S. de Gironcoli, S. Fabris, G. Fratesi, R. Gebauer, U. Gerstmann, C. Gougoussis, A. Kokalj, M. Lazzeri, L. Martin-Samos, N. Marzari, F. Mauri, R. Mazzarello, S. Paolini, A. Pasquarello, L. Paulatto, C. Sbraccia, S. Scandolo, G. Sclauzero, A. P. Seitsonen, A. Smogunov, P. Umari and R. M. Wentzcovitch, *J. Phys. Condens. Matter*, 2009, **21**, 395502.
21 M. Valiev, E. J. Bylaska, N. Govind, K. Kowalski, T. P. Straatsma, H. J. J. V. Dam, D. Wang, J. Nieplocha, E. Apra, T. L. Windus and W. A. D. Jong, *Comput. Phys. Commun.*, 2010, **181**, 1477–1489.
22 D. M. Deaven and K. M. Ho, *Phys. Rev. Lett.*, 1995, **75**, 288–291.
23 F. Stienkemeier, J. Higgins, W. E. Ernst and G. Scoles, *Zeitschrift für Phys. B Condens. Matter*, 1995, **98**, 413–416.
24 C. B. Murray, D. J. Norris and M. G. Bawendi, *J. Am. Chem. Soc.*, 1993, **115**, 8706–8715.
25 D. Norris and M. Bawendi, *Phys. Rev. B*, 1996, **53**, 16338–16346.
26 V. N. Soloviev, A. Eichhöfer, D. Fenske and U. Banin, *Phys. Status Solidi Basic Res.*, 2000, **224**, 285–289.
27 J. Jasieniak, M. Califano and S. E. Watkins, *ACS Nano*, 2011, **5**, 5888–5902.
28 X. Gao, Y. Cui, R. M. Levenson, L. W. K. Chung and S. Nie, *Nat. Biotechnol.*, 2004, **22**, 969–976.
29 P. V. Kamat, *J. Phys. Chem. C*, 2008, **112**, 18737–18753.
30 V. I. Klimov, *Science*, 2000, **290**, 314–317.
31 F. Zhang, S. Wang, L. Wang, Q. Lin, H. Shen, W. Cao, C. Yang, H. Wang, L. Yu, Z. Du, J. Xue and L. S. Li, *Nanoscale*, 2016, **8**, 12182–12188.
32 Y. E. Panfil, M. Oded and U. Banin, *Angew. Chemie - Int. Ed.*, 2018, **57**, 4274–4295.
33 K. A. Nguyen, P. N. Day and R. Pachter, *J. Phys. Chem*, 2010, **114**, 16197–16209.
34 R. Nadler and J. F. Sanz, *Theor. Chem. Acc.*, 2013, **132**, 1342.
35 S. A. Fischer, A. M. Crotty, S. V. Kilina, S. A. Ivanov and S. Tretiak, *Nanoscale*, 2012, **4**, 904–914.
36 S.-P. Yu, D.-L. Huang, Z.-G. Zhao, M.-L. Yang and M.-H. Yang, *J. Clust. Sci.*, 2017, **28**, 1825.
37 J. M. Azpiroz, J. M. Matxain, I. Infante, X. Lopez and J. M. Ugalde, *Phys. Chem. Chem. Phys.*, 2013, **15**, 10996–1005.
38 S. Xu, C. Wang and Y. Cui, *J. Mol. Model.*, 2010, **16**, 469–473.
39 J. P. Perdew, K. Burke, M. Ernzerhof, D. of Physics and N. O. L. . J. Quantum Theory Group Tulane University, *Phys. Rev. Lett.*, 1996, **77**, 3865–3868.
40 A. M. Rappe, K. M. Rabe, E. Kaxiras and J. D. Joannopoulos, *Phys. Rev. B*, 1990, **41**, 1227–1230.
41 C. Adamo and V. Barone, *J. Chem. Phys.*, 1999, **110**, 6158–6170.
42 W. J. Stevens, M. Krauss, H. Basch and P. G. Jasien, *Can. J. Chem*, 1992, **70**, 612.
43 G. Kresse and D. Joubert, *Phys. Rev. B*, 1999, **59**, 1758–1775.
44 E. Sanville, A. Burnin and J. J. BelBruno, *J. Phys. Chem. A*, 2006, **110**, 2378–2386.
45 K. A. Peterson, *J. Chem. Phys.*, 2003, **119**, 11099–11112.
46 K. A. Peterson and C. Puzzarini, *Theor. Chem. Acc.*, 2005, **114**, 283–296.
47 M. Jäger, A. Shayeghi, V. Klippenstein, R. L. Johnston and R. Schäfer, *J. Chem. Phys.*, 2018, **149**, 244308.
48 P. Yang, S. Tretiak, A. E. Masunov and S. Ivanov, *J. Chem. Phys.*, 2008, **129**, 074709.
49 M. Del Ben, R. W. A. Havenith, R. Broer and M. Stener, *J. Phys. Chem. C*, 2011, **115**, 16782–16796.
50 E. Antolini, T. Lopes and E. R. Gonzalez, *J. Alloys Compd.*, 2008, **461**, 253–262.
51 C. Wang, H. Daimon, T. Onodera, T. Koda and S. Sun, *Angew. Chemie - Int. Ed.*, 2008, **47**, 3588–3591.
52 C. T. Campbell, *Nat. Chem.*, 2012, **4**, 597–598.
53 G. Kim, Y. Kawazoe and K. R. Lee, *J. Phys. Chem. Lett.*, 2012, **3**, 1989–1996.
54 J. Klett, S. Krähling, B. Elger, R. Schäfer, B. Kaiser and W. Jaegermann, *Zeitschrift fur Phys. Chemie*, 2014, **228**, 503–520.
55 S. C. Ammal and A. Heyden, *ACS Catal.*, 2014, **4**, 3654–3662.
56 S. Vajda, M. J. Pellin, J. P. Greeley, C. L. Marshall, L. A. Curtiss, G. A. Ballentine, J. W. Elam, S. Catillon-Mucherie, P. C. Redfern, F. Mehmood and P. Zapol, *Nat. Mater.*, 2009, **8**, 213–216.
57 K. Koszinowski, D. Schröder and H. Schwarz, *J. Phys. Chem. A*, 2003, **107**, 4999–5006.
58 C. Adlhart and E. Uggerud, *Chem. Commun.*, 2006, 2581–2582.
59 O. P. Balaj, I. Balteanu, T. T. Roßteuscher, M. K. Beyer and V. E. Bondybey, *Angew. Chemie - Int. Ed.*, 2004, **43**, 6519–6522.
60 L. Xin, F. Yang, S. Rasouli, Y. Qiu, Z. F. Li, A. Uzunoglu, C. J. Sun, Y. Liu, P. Ferreira, W. Li, Y. Ren, L. A. Stanciu and J. Xie, *ACS Catal.*, 2016, **6**, 2642–2653.
61 G. Ramos-Sanchez and P. B. Balbuena, *Phys. Chem. Chem. Phys.*, 2013, **15**, 11950–11959.
62 T. Yumura, T. Awano, H. Kobayashi and T. Yamabe, *Molecules*,

This journal is © The Royal Society of Chemistry [year]

2012, **17**, 7941–7960.
63 J. A. Santana and N. Rösch, *J. Phys. Chem. C*, 2012, **116**, 10057–10063.
64 X. Wang and D. Tian, *Comput. Mater. Sci.*, 2009, **46**, 239–244.
65 A. S. Chaves, G. G. Rondina, M. J. Piotrowski, P. Tereshchuk and J. L. Da Silva, *J. Phys. Chem. A*, 2014, **118**, 10813–10821.
66 S. Winczewski and J. Rybicki, *Comput. Methods Sci. Technol.*, 2011, **17**, 75–85.
67 Y. Akdogan, S. Anantharaman, X. Liu, G. Lahiri, H. Bertagnolli and E. Roduner, *J. Phys. Chem. C*, 2009, **113**, 2352–2359.
68 R. L. T. Parreira, G. F. Caramori, S. E. Galembeck and F. Huguenin, *J. Phys. Chem. A*, 2008, 11731.
69 P. C. Jennings and R. L. Johnston, *Comput. Theor. Chem.*, 2013, **1021**, 91–100.
70 F. Weigend and R. Ahlrichs, *Phys. Chem. Chem. Phys.*, 2005, **7**, 3297–3305.